UC Santa Cruz

UC Santa Cruz Previously Published Works

Title

Highly stable preferential carbon monoxide oxidation by dinuclear heterogeneous catalysts

Permalink

https://escholarship.org/uc/item/4j13m1ks

Journal

Proceedings of the National Academy of Sciences of the United States of America, 120(1)

ISSN

0027-8424

Authors

Zhao, Yanyan
Dai, Sheng
Yang, Ke R
et al.

Publication Date

2023-01-03

DOI

10.1073/pnas.2206850120

Peer reviewed

eScholarship.org Powered by the California Digital Library
University of California

PNAS RESEARCH ARTICLE | CHEMISTRY

Highly stable preferential carbon monoxide oxidation by dinuclear heterogeneous catalysts

Yanyan Zhao[a,1], Sheng Dai[b,1], Ke R. Yang[c,1], Sufeng Cao[a,d], Kelly L. Materna[c], Hannah M. C. Lant[c], Li Cheng Kao[e], Xuefei Feng[e], Jinghua Guo[e], Gary W. Brudvig[c], Maria Flytzani-Stephanopoulos[d], Victor S. Batista[c,2], Xiaoqing Pan[b,2], and Dunwei Wang[a,2]

Edited by Eric A. Stach, University of Pennsylvania, Philadelphia, PA; received April 19, 2022; accepted November 9, 2022 by Editorial Board Member Joanna Aizenberg

Atomically dispersed catalysts have been shown highly active for preferential oxidation of carbon monoxide in the presence of excess hydrogen (PROX). However, their stability has been less than ideal. We show here that the introduction of a structural component to minimize diffusion of the active metal center can greatly improve the stability without compromising the activity. Using an Ir dinuclear heterogeneous catalyst (DHC) as a study platform, we identify two types of oxygen species, interfacial and bridge, that work in concert to enable both activity and stability. The work sheds important light on the synergistic effect between the active metal center and the supporting substrate and may find broad applications for the use of atomically dispersed catalysts.

preferential CO oxidation | catalysis | iridium

Significance

We have carried out atomically resolved STEM observations of catalyst behaviors in operando. The data intuitively illustrate how dinuclear catalysts are more stable than single atom ones under the reaction conditions. Ourresults shed new light on the role of different oxygen atoms near the active center. An oxygen atom that links asingle atom catalyst and the supporting substrate often plays multiple roles. Through extensive computationalefforts, in concert with experimental verifications, we learned that bridge oxygen mainly serves to stabilize thecatalyst, while interfacial oxygen acts as the participant in the chemical processes for activity. The knowledgeis expected to be broadly impactful to the community.

Preferential CO oxidation in the presence of excess H_2 (PROX) promises a route to removing CO as a key contaminant in H_2 for a wide range of applications (1). Significant research has been attracted to carrying out PROX at low temperatures (e.g., <200 °C) so as to maximize the selectivity toward CO removal rather than H_2 oxidation (2). Driven by the understanding that strong CO binding between adjacent metal atoms in metallic nanoparticles (NPs) would block the active site, which leads to inferior activity, much of the recent attention has been directed toward studying atomically dispersed catalysts. Indeed, exciting progress has been made. Outstanding per atom catalytic activity, for example, has been reported on Pt single-atom catalysts (SACs) dispersed on a variety of supports (3, 4). Moving forward, how to maintain the high activity for prolonged operations becomes a critical issue that has received relatively little attention. The handful of studies that address the stability issue of atomically dispersed catalysts describe a strong dependence of such stability on the substrate support (5, 6). That is, the interactions between the metal active center and the supporting substrate (often metal oxides) are critical to the performance of the atomically dispersed catalysts (7, 8). While intuitive, this observation raises critical new questions concerning the mechanisms by which PROX proceeds on a single-atom site (9). A growing body of evidence suggests that the synergistic effect between the active center and the substrate, mediated by the interfacial atoms (often O-based species), is of vital importance (10–14). However, while the pivotal role played by interfacial O atoms toward activity has been inferred in the literature (15), the implications of these species to the stability of the catalyst under operating conditions are not fully understood. More importantly, it still has a knowledge gap on how to capitalize on the existing knowledge to achieve atomically dispersed catalysts that are both active and stable. Here, we report a study aimed at filling this gap. Using a combination of super high-resolution in situ imaging and density functional theory (DFT) calculations, we identified two types of O atoms, bridge and interfacial, in the atomically dispersed dinuclear Ir catalysts (Fig. 1*A*). It was found that outstanding stability can be afforded by the bridge O atom between two active metal centers, whereas the activity was mainly connected to the interfacial O atom between the active center and the supporting substrate. These results shed important light on the principles governing the stability and activity of atomically dispersed catalysts.

This study was enabled by a unique study platform, the Ir dinuclear heterogeneous catalysts (DHCs) on CeO_2. It features an active center consisting of two Ir atoms, linked and separated by bridge O species. The unit is anchored onto the CeO_2 support by interfacial O species (Fig. 1*A* and *SI Appendix*, Figs. S1 and S2). More details about the preparation are provided in the *SI Appendix*. As shown in Fig. 1*B* and *SI Appendix*, Fig. S3, the dinuclear nature is most directly revealed by ex situ aberration-corrected scanning transmission electron microscopy (AC-STEM). The high angle annular dark field-STEM (HAADF-STEM) image as shown in Fig. 1*B* was taken along the [10$\bar{1}$] zone axis of CeO_2. Notably, under this specific condition with UV treatment for 20 min after immersing the CeO_2 in an Ir dimer precursor

Author contributions: D.W. designed research; Y.Z., S.D., K.R.Y., and S.C. performed research; K.L.M., H.M.C.L., X.F., J.G., M.F.-S., V.S.B., and X.P. contributed new reagents/analytic tools; Y.Z., K.R.Y., L.C.K., G.W.B., V.S.B., and D.W. analyzed data; and Y.Z., K.R.Y., and D.W. wrote the paper.

The authors declare no competing interest.

This article is a PNAS Direct Submission. E.A.S. is a guest editor invited by the Editorial Board.

Copyright © 2022 the Author(s). Published by PNAS. This article is distributed under Creative Commons Attribution-NonCommercial-NoDerivatives License 4.0 (CC BY-NC-ND).

[1]Y.Z., S.D., and K.R.Y. contributed equally to this work.

[2]To whom correspondence may be addressed. Email: victor.batista@yale.edu, xiaoqinp@uci.edu, or dunwei.wang@bc.edu.

This article contains supporting information online at https://www.pnas.org/lookup/suppl/doi:10.1073/pnas.2206850120/-/DCSupplemental.

Published December 28, 2022.

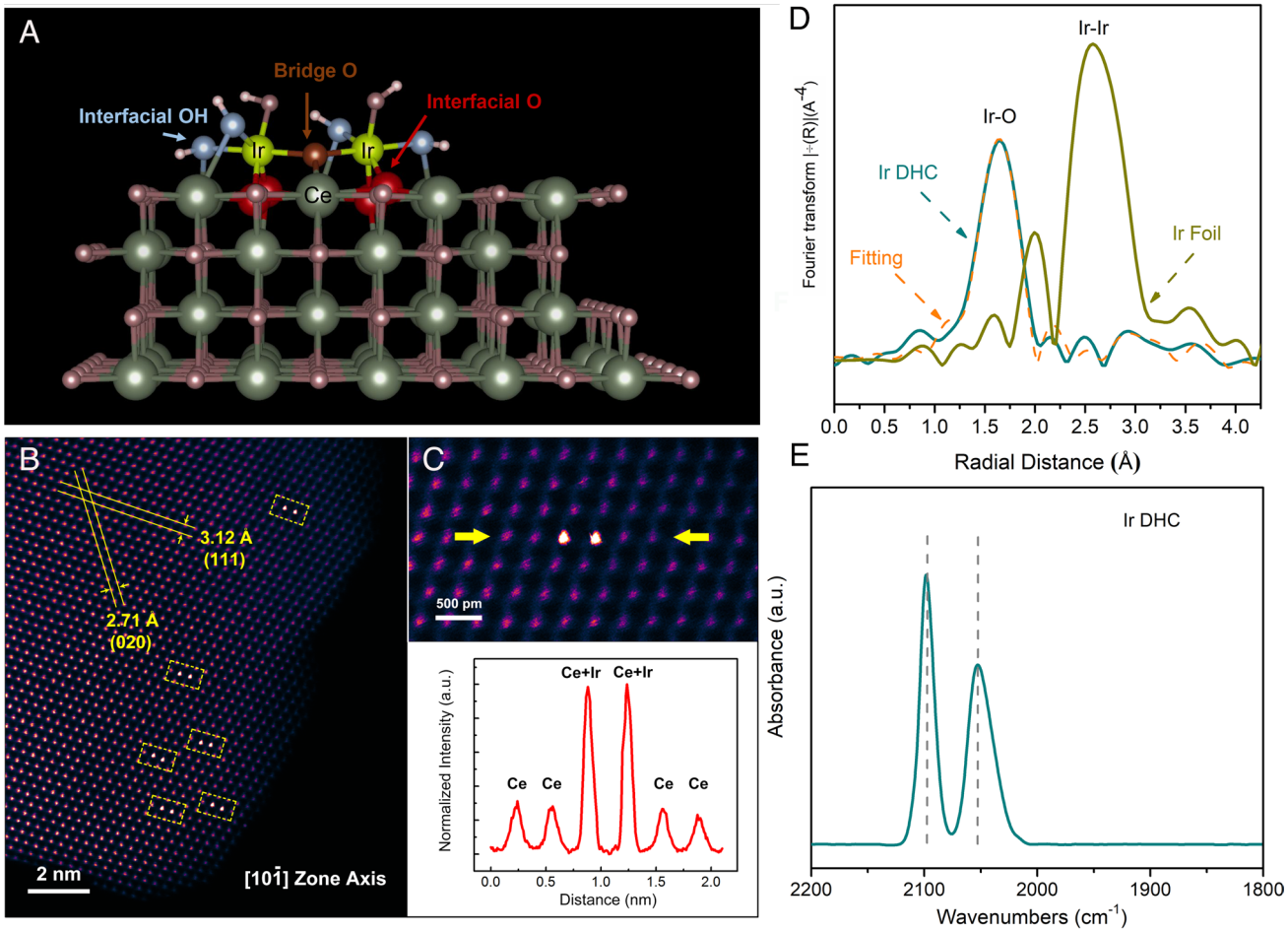

Fig. 1. Direct characterization of Ir DHC/CeO_2 catalyst. (*A*) DFT optimized the minimum energy structure of Ir DHC on CeO_2 (side view). The yellow and green balls indicate Ir and Ce; the blue, brown, red, and brandy rose balls represent interfacial OH, bridge O atoms, interfacial O atoms, and O atoms in the bulk and other environments, respectively. (*B*) A false-colored HAADF-STEM image of Ir DHC/CeO_2 along the [10$\bar{1}$] zone axis of CeO_2, where the Ir atoms are highlighted (within yellow dashed rectangles). (*C*) A magnified view of a single Ir DHC on CeO_2. Normalized intensity profile taken along the line indicated by the yellow arrows. (*D*) EXAFS experimental and fitted spectra based on the DFT atomic model of Ir DHC on CeO_2 and bulk Ir foil at the Ir L-edge. (*E*) In situ DRIFTS spectra of Ir DHCs.

solution (16, 17), we observed Ir heterogeneous atoms in pairs. In Fig. 1*C*, a single pair was examined (*Top*), where a line scan of the Z-contrast (*Bottom*) permitted the measurement of the atomic spacing between the two Ir atoms at ca. 3.7 Å. This value is in excellent agreement with the DFT-optimized structure model as shown in Fig. 1*A*, where Ir atoms are coordinated by O atoms with an average Ir–O distance of 2.0 Å, and the two Ir centers are connected by a mono-μ-oxo bridge with an Ir–Ir distance of 3.7 Å (Ir–O–Ir). The structure of the Ir DHCs was further studied by extended X-ray absorption fine structure spectroscopy (EXAFS) and diffuse reflectance infrared Fourier transform spectroscopy (DRIFTS). The EXAFS data shown in Fig. 1*D* provided strong support to the DFT structure model, which is evidenced by the good match between the simulated and experimental spectra. The presence of Ir–O bonds in the first coordination shell as well as an Ir–O–Ir and Ir–O–Ce interaction in the second coordination shell from the EXAFS simulation (*SI Appendix*, Fig. S4 and Table S2) also confirmed that there were no significant byproducts such as nanoscale clusters (often referred to as NPs). The homogeneity of the Ir DHCs on CeO_2 was also further supported by the DRIFTS spectra (Fig. 1*E*). Two characteristic singlet peaks at 2,098 and 2,052 cm^{-1} can be ascribed to the asymmetric and symmetric stretching of the CO probe on Ir DHC, respectively. Together, this set of data demonstrates that we have successfully obtained monodispersed Ir DHCs on CeO_2, whose structure is resolved as shown in Fig. 1*A*.

With the structural information confirmed, we next performed PROX using Ir DHCs on CeO_2 at 453 K (Fig. 2*A*). As an important control, Ir SACs with well-defined structures (*SI Appendix*, Fig. S5) were also prepared and subjected to similar catalytic conditions. It was observed that while Ir DHCs and SACs exhibited comparable initial activity, the main benefit of Ir DHCs was outstanding durability, with 7% decay for the first 120 h. In contrast, only 75% of the initial activity was measured on Ir SACs at 40 h, which further decreased to 63% after 120 h.

To help us better understand the stability exhibited by Ir DHCs, we compared our catalyst with various other recently reported catalysts by using 5% decay of CO conversion as a benchmark. It is obvious from *SI Appendix*, Fig. S6 that our catalyst is among the best (2, 3, 11, 18, 19). It is cautioned that the detailed structures of the reported catalysts, their inherent activities, as well as the test conditions, tend to vary greatly; moreover, a protocol that allows for unbiased, direct comparison is not yet available. Even with these constraints in mind, we can clearly see the outstanding performance exhibited by Ir DHCs in both activity and stability. Most strikingly, the Ir DHCs were much more stable than Ir SACs despite similar synthesis conditions, almost identical loading amounts of active elements, and the same supporting substrate. Characterization of the Ir DHC and SAC after the reaction was carried out. A negligible change was observed for the Ir DHC (*SI Appendix*, Fig. S7), whereas the features characteristic of Ir NPs

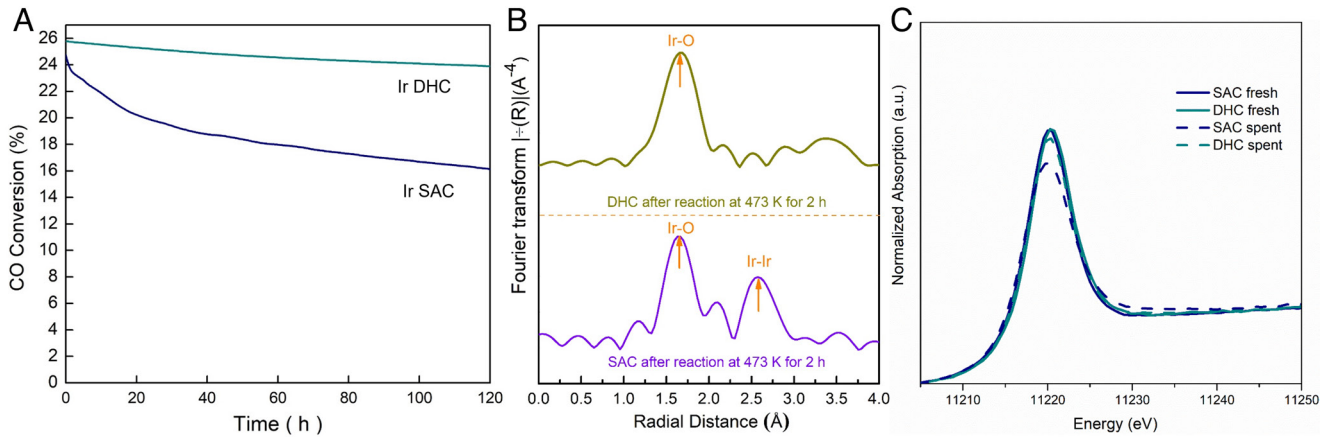

Fig. 2. Catalytic stability characterization: (*A*) CO PROX stability test over Ir DHC and SAC on CeO_2. Reaction conditions: 40 mL/min flow rate, 1% CO, 1% O_2, 40% H_2, bal. He, 50 mg catalyst loading, T = 453 K; (*B*) In situ EXAFS and (*C*) XANES spectra of Ir DHC and SAC. Reaction conditions: 20 mL/min flow rate, 1% CO, 1% O_2, 40% H_2, bal. He, 473 K, 2 h, ~10 mg catalyst loading.

can be found in Ir SAC samples after the reaction (*SI Appendix*, Fig. S8). The result suggests that significant Ir aggregation took place for the Ir SAC but not for the Ir DHC. Intrigued by the observation, we were prompted to ask the following question: What is the key difference between DHCs and SACs that leads to such a stark contrast in their stability?

Answers to this research question have significant implications. While a range of SACs has been shown active toward PROX, a critical question remains unanswered. It concerns the mechanism by which O_2 is activated by the single-atom site where CO is also strongly bonded. The most compelling working hypothesis invokes the participation of various O species such as the interfacial O, which serves to anchor the single-atom site to the supporting oxide or the lattice O that is part of the supporting substrate or both (20–22). The Ir DHCs are different from Ir SACs and, by extension of structural similarities, many reported SACs of other compositions, in that they feature additional O species like the bridge O (Fig. 1*A*). Moreover, the close vicinity of a second Ir atom that is not directly bonded with Ir (i.e., no metal–metal interactions) might enable synergistic effects for simultaneous O_2 and CO activation. We are, therefore, encouraged to explore two new possibilities: 1) Bridge O may enhance the stability of atomically dispersed active sites and 2) synergistic effects between adjacent Ir atoms may promote PROX. As will be discussed next, our results confirmed the former but ruled out the latter.

To test the first possibility, we have examined the structural changes of Ir SACs and DHCs during the PROX reaction. While no significant difference was observed between the EXAFS spectra for Ir DHCs before (Fig. 1*D*) and after PROX (Fig. 2*B*), a rise of the peak that is indicative of Ir–Ir bonding became apparent for Ir SACs under in operando XAS at 473 K (ambient pressure, 1% CO, 1% O_2, 40% H_2 balanced by He). The aggregation of Ir SAC was also validated by X-ray absorption near edge spectroscopy (XANES) spectra (Fig. 2*C*), which supported that the average valence state of Ir in Ir SACs decreased. This set of data implies that agglomeration of Ir SACs took place during PROX. Under identical conditions, similar changes were not observed for Ir DHCs. From the structural models of Ir DHC and SAC, both Ir SAC and DHC are anchored on the surface by interfacial O species (OH and O), while Ir DHC has one additional bridge O atom to hold the two Ir together (Fig. 1*A*). During reactions, the formal oxidation state of Ir in SAC is reduced to +1, whereas those in DHC are in mixed valences of +1 and +3, which was also validated by XANES. Of them, the Ir^+ acts to activate O_2 for CO oxidation, and the Ir^{3+}, which is coordinatively stable, provides the structural stability to prevent the DHC from moving around.

To obtain direct evidence that supports this understanding, we carried out in situ AC-STEM observations by placing Ir DHCs and SACs inside a TEM nanoreactor and exposed them to CO gas (760 Torr of 5% CO, *SI Appendix*, Figs. S9 and S10) and a CO/H_2 gas mixture (400 Torr of 5% H_2 and 10 Torr of 5% CO, Fig. 3 *A* and *B*), respectively, at 473 K. In these experiments, internal features of CeO_2 (such as grain boundaries in Fig. 3*B*) were used as alignment marks for locating the relative positions of the individual Ir DHCs and SACs. A control experiment under pure N_2 showed negligible electron beam effect of image acquisition on the Ir species (*SI Appendix*, Fig. S11 and associated discussions therein) (23). Under conditions similar to PROX (400 Torr of 5% H_2 and 10 Torr of 5% CO), a diffusion of 15.4 Å was observed for Ir SACs within the first 5 min; then, an additional diffusion distance of 16.2 Å was measured between 5 min and 10 min (Fig. 3*B*). By contrast, no measurable movement was observed for Ir DHCs under the same conditions for 60 min (Fig. 3*A*). It is noted that the strong binding of CO has been previously reported to weaken the anchoring of SACs on metal oxide supports (24). Our DFT calculations support the observation, too. It is seen in Fig. 3*C* and *SI Appendix*, Figs. S12 and S13 that the diffusion of Ir SACs on the CeO_2 (110) facet is an isothermal process with an estimated activation energy of 1.6 eV, indicating that diffusion is highly possible. The detachment of Ir DHCs on CeO_2, however, incurs a significant thermodynamic penalty of ca. 4.9 eV, making detachment an unlikely pathway (Fig. 3*D*). Diffusion of Ir DHCs as a whole is highly unlikely due to the requirement of breaking six Ir–O bonds simultaneously. Therefore, we considered a stepwise diffusion process, where the Ir^+ center diffuses first to lead to the breaking of the Ir–O–Ir structural motif; this process would incur a 1.6 eV increase of the thermodynamic energy with an estimated activation energy of 3.2 eV (Fig. 3*E*) and is also unlikely. A more likely route by which Ir DHCs can be removed from the surface would be the initial dissociation of the two Ir ions on the surface. Indeed, by exposing the Ir DHC under intentionally strong electron beam irradiation in the vacuum chamber during the AC-STEM observation, we only observed dissociation of Ir DHCs, which led to the formation of Ir SACs that exhibited diffusion behaviors subsequently (*SI Appendix*, Fig. S14). It is conceivable that the diffusion of Ir SACs would lead to eventual aggregations that form Ir NPs (*SI Appendix*, Fig. S15), which would help to explain the

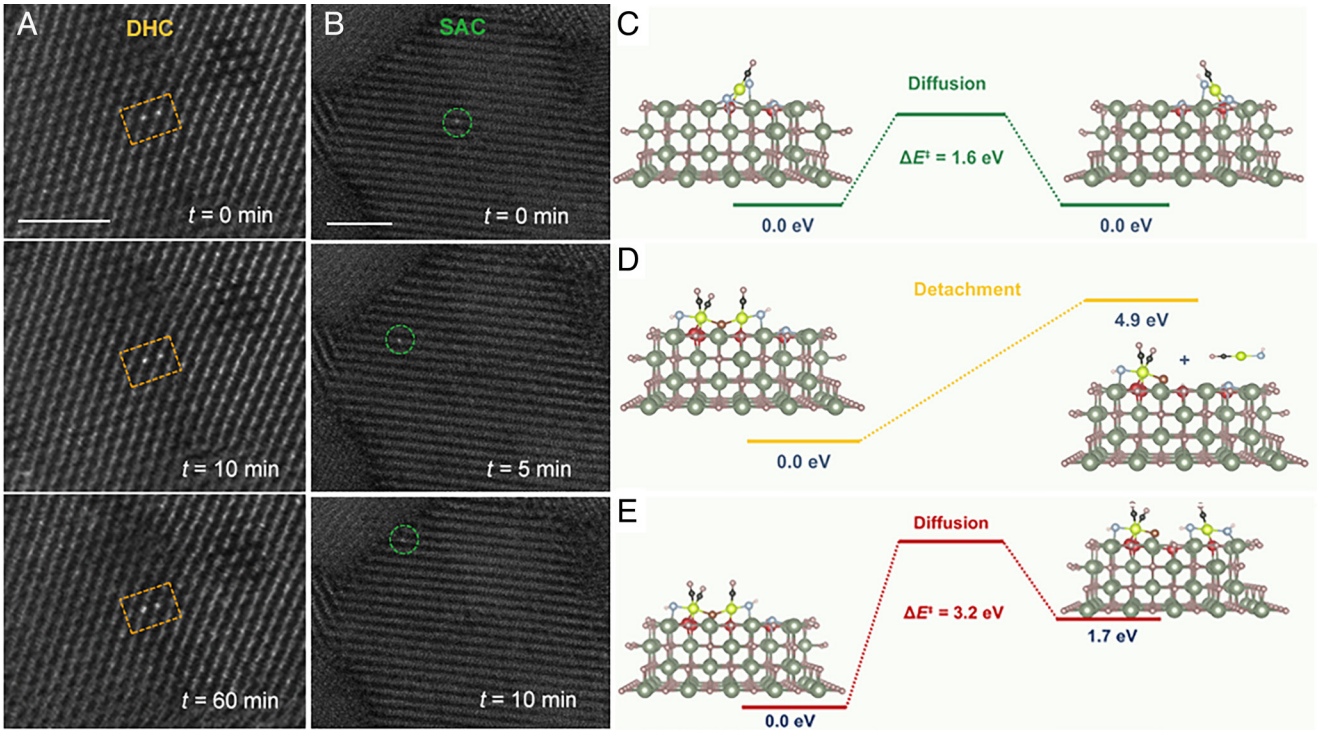

Fig. 3. Direct stability observation. In situ AC-STEM characterization of Ir DHC/CeO_2 under gas-phase condition. In situ HAADF-STEM images showing the mobility of Ir DHC (*A*) and SAC (*B*) with the gas phase (400 Torr of 5% H_2 + 10 Torr of 5% CO, 473 K) to mimic the PROX condition (Scale bar, 2 nm.) The colored circles highlight the same Ir SAC and Ir DHC. Calculated reaction energy changes (ΔE) and associated barrier height ($\Delta E^{\ddagger}$) for (*C*) diffusion of Ir SAC, (*D*) detachment of Ir DHC and (*E*) diffusion of Ir DHC on CeO_2 surface assisted by one CO.

spectroscopic features observed in Fig. 2*B*. The understanding is also confirmed by STEM and DRIFTS data for postreaction samples (*SI Appendix*, Fig. S8). Taken as a whole, this set of data confirms that the dinuclear nature of the Ir DHCs greatly enhances their stability as compared with SACs. With bridge O being the key differentiating feature between Ir DHCs and SACs, it is concluded that the stability directly benefits from the presence of this species. Next, we will demonstrate that bridge O indeed does not participate in the catalytic cycles.

A growing body of literature on SACs-based PROX or CO oxidation supports that interfacial O plays a critical role in the catalytic cycle. The working hypotheses often involve the combination of interfacial O with adsorbed CO, resulting in CO_2 as a leaving product and an O vacancy to be replenished by adsorbed O_2, which completes the catalytic cycle. When examining the structural details of Ir DHCs and SACs, we propose that the same function could be played by bridge O, as well, in which case a fundamental difference would be expected in the apparent activation energies of the overall reactions. To test this possibility, we next performed CO oxidation at varying temperatures (Fig. 4*A*). CO was already converted to CO_2 by Ir DHC at temperatures as low as 373 K and was almost depleted at 453 K. A kinetic study was carried out in the kinetically controlled region (<20% conversion) to construct the Arrhenius plots as shown in Fig. 4*B*. The apparent activation energies for Ir DHCs and SACs were nearly identical. As such, CO oxidation might proceed on the two types of catalysts following similar mechanisms or share a common step that determines the activation energy, which would invoke the participation of interfacial O but not bridge O.

The understanding is strongly supported by computational studies of the catalytic cycle (25, 26), the results of which are detailed in Fig. 4*C* and *SI Appendix*, Figs. S16–S21 and Tables S3–S7. Our proposed catalytic mechanism starts with a di-carbonyl intermediate **I** that features 2 Ir^{3+} centers connected by a bridge O atom, as suggested by in situ DRIFTS spectra and computational study of Ir SAC and DHC under H_2 and CO atmosphere. As shown in Fig. 4*C*, there are interfacial O species (O and OH) and a bridge O atom in intermediate **I**. Therefore, there are three possible pathways for CO to react with the nearby O atoms. As shown in *SI Appendix*, Fig. S19, only when the CO couples with an interfacial O atom, the reaction is exothermic, forming a five-coordinated Ir center with a chemically adsorbed CO_2 (intermediate **II**). Intermediate **II** releases a CO_2 molecule to form a mixed-valent intermediate **III** with one Ir in oxidation state (III) and one Ir in oxidation state (I). The four-coordinated Ir^+ center has a square-planar geometry, a typical geometry for an Ir^+ complex (25). The overall process from intermediate **I** to intermediate **III** is a typical reductive elimination reaction of Ir^{3+} complexes. As highlighted in Fig. 4*C*, intermediate **III** has an oxygen vacancy near the Ir^+ center which was previously occupied by an interfacial O atom. The oxygen vacancy in intermediate **III** can bind to an O_2 molecule at the Ir^+ center with an energy change of −1.02 eV to form intermediate **IV**, which undergoes O–O cleavage to form intermediate **V** with an Ir^{4+}–O unit. A CO molecule from the gas phase can be physically adsorbed by intermediate **V**, forming intermediate **VI** and then oxidized to CO_2 and intermediate **VII** (27) with a large energy change of −2.06 eV. The release of the second CO_2 in intermediate **VII** generates intermediate **VIII** with a coordinatively unsaturated Ir^{3+} center, which can be replenished by a CO molecule from the gas phase to complete the catalytic cycle. In the proposed catalytical cycle, we were able to locate two transition states: one for CO reaction with an interfacial O atom to form CO_2 (**TS1** between intermediates **I** and **II**) and one for the O–O cleavage to activate O_2 (**TS2** connects intermediates **IV** and **V**). The oxidation of the first CO molecule is the rate-determining step (rds) with a calculated activation energy of 0.78

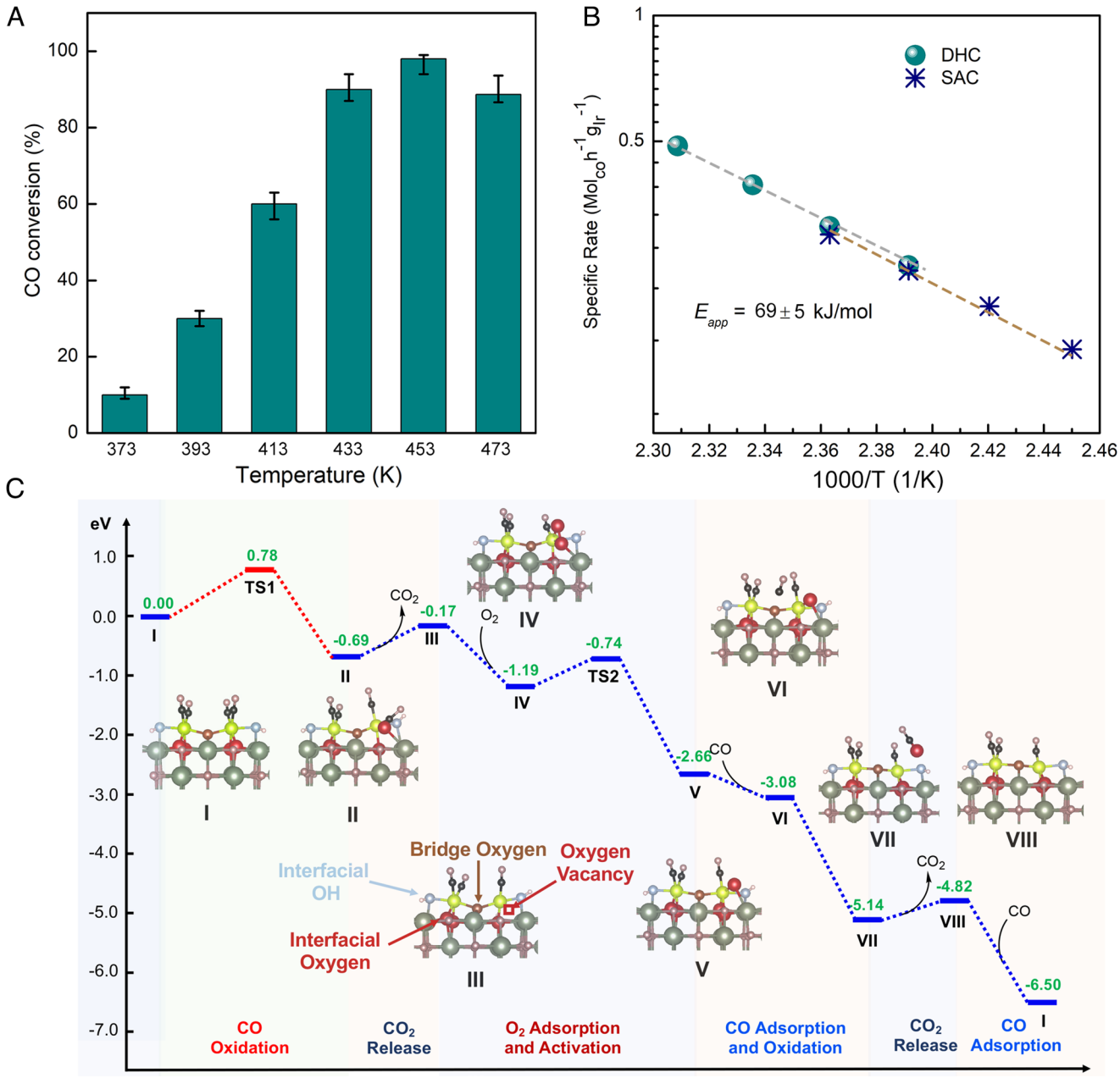

Fig. 4. Low-temperature activity initiated by interfacial oxygen. (*A*) CO conversion by Ir DHC for CO PROX reaction at different temperatures. Test conditions: 30 mL/min flow rate, 1% CO, 1% O_2, 40% H_2, bal. He, 250 mg catalyst loading. (*B*) Arrhenius-type plot of CO PROX reaction over Ir SAC and DHC. Test conditions: 100 mL/min flow rate, 1% CO, 1% O_2, 40% H_2, bal. He, 100 mg catalyst loading, conversion of CO is controlled below 20% to be in the kinetic region. (*C*) The reaction pathway of catalytic CO oxidation over Ir DHC on CeO_2 suggested by DFT calculations. The vertical axis shows the relative energies of intermediates and transition states in the unit of eV. The DFT-optimized structures of intermediates are shown with labels associated with them.

eV, consistent with the experimentally measured apparent activation energy.

In the proposed catalytic cycle, an O vacancy is generated in situ through the oxidation of the first CO molecule by an interfacial O atom, which activates gas phase O_2 between the Ir^+ center and CeO_2 surface to oxidize the second CO molecule and replenish the interfacial oxygen. Intermediate **III** is a mixed-valent Ir dimer with one Ir in oxidation state 3+ and one in oxidation state 1+. It is highly unlikely to have both Ir^{3+} being reduced to Ir^+ under reaction conditions since the replenishment of the O vacancy by O_2 is highly exothermic and thermodynamically favorable (Fig. 4*C*). More discussions about the mechanism are provided in the *SI Appendix*. It is emphasized here that only one Ir center in the DHC and the interfacial O are involved in the catalytic cycle, accounting for the high activity of both Ir SAC and DHC and their similar energy profile along the reaction path (*SI Appendix*, Fig. S20), whereas the bridging O atom serves to hold the two Ir centers together and the other Ir provides strong anchoring to the substrate. Together, the DHC affords superior stability without compromising activity.

In conclusion, two types of O species are identified for atomically dispersed Ir catalysts. The first is interfacial O which connects the active metal center to the substrate. It participates in the PROX reaction by adsorbing O_2 and oxidizing CO and may be considered a critical component for the reactivity. Similar O species are abundant in SACs, which may help explain the high activity that has

been reported on these catalysts. The second type of O species bridges two metal active centers and is independent of the metal–substrate interactions. There is no evidence that bridge O participates in the catalytic cycles of PROX. Rather, bridge O mainly helps to minimize diffusion of the metal active centers to afford outstanding stability. Building on the recent successes in achieving high activity on atomically dispersed catalysts, our results imply that introducing structural components may contribute significantly to the eventual goal of achieving catalysts that are both active and stable.

Code Availability Statement. The computer code and algorithm generated during and/or analyzed during the current study have been included in the *SI Appendix*.

Data, Materials, and Software Availability. The datasets generated during and/or analyzed during the current study have been included in the manuscript or the *SI Appendix*.

ACKNOWLEDGMENTS. The project was mainly supported by the National Science Foundation (CHE 1955098 to Boston College, CHE 1955237 to Yale, and CHE 1955786 to UC Irvine). We also thank an Ignite grant from Boston College for catalyst synthesis and catalytic characterization; precursor synthesis and theoretical computations at Yale University were also supported by the Center for Light Energy Activated Redox Processes (LEAP), an Energy Frontier Research Center funded by the US Department of Energy (DOE), Office of Science, Office of Basic Energy Sciences (BES), under Award DE-SC0001059. K.R.Y. and V.S.B. acknowledge the computer time from the National Energy Research Scientific Computing Center (NERSC) and Yale Center for Research Computing (YCRC). *Ex-situ*XAS used resources of the Advanced Light Source, a DOE Office of Science User Facility under contract no. DE-AC02-05CH11231. We thank Zechao Wang for helping with HAADF-STEM. Sufeng Cao thanks Dr. Sungsik Lee for helping with x-ray absorption spectroscopy (XAS) data acquisition. We thank Dr. Sirine Fakra for helping with XAS data acquisition.

Author affiliations: [a]Department of Chemistry, Merkert Chemistry Center, Boston College, Chestnut Hill, MA 02467; [b]Department of Physics and Astronomy, University of California–Irvine, Irvine, CA 92697; [c]Yale Energy Sciences Institute and Department of Chemistry, Yale University, New Haven, CT 06520; [d]Department of Chemical and Biological Engineering, Tufts University, Medford, MA 02155; and [e]Advanced Light Source, Lawrence Berkeley National Laboratory, Berkeley, CA 94720

1. K. Liu, A. Wang, T. Zhang, Recent advances in preferential oxidation of CO reaction over platinum group metal catalysts. *ACS Catalysis* **2**, 1165–1178 (2012).
2. L. Cao *et al.*, Atomically dispersed iron hydroxide anchored on Pt for preferential oxidation of CO in H2. *Nature* **565**, 631–635 (2019).
3. B. Qiao *et al.*, Single-atom catalysis of CO oxidation using Pt1/FeOx. *Nat. Chem.* **3**, 634–641 (2011).
4. Z. Zhang *et al.*, Thermally stable single atom Pt/m-Al2O3 for selective hydrogenation and CO oxidation. *Nat. Commun.* **8**, 16100 (2017).
5. P. Hu *et al.*, Electronic metal-support interactions in single-atom catalysts. *Angew. Chem. Int. Ed. Engl.* **53**, 3418–3421 (2014).
6. J.-C. Liu, Y. Tang, Y. G. Wang, T. Zhang, J. Li, Theoretical understanding of the stability of single-atom catalysts. *Nat. Sci. Rev.* **5**, 638–641 (2018).
7. T. Kropp, Z. Lu, Z. Li, Y.-H.C. Chin, M. Mavrikakis, Anionic single-atom catalysts for CO oxidation: Support-independent activity at low temperatures. *ACS Catalysis* **9**, 1595–1604 (2019).
8. B. Qiao *et al.*, Ultrastable single-atom gold catalysts with strong covalent metal-support interaction (CMSI). *Nano Res.* **8**, 2913–2924 (2015).
9. B. Qiao *et al.*, Highly efficient catalysis of preferential oxidation of CO in H2-rich stream by gold single-atom catalysts. *ACS Catalysis* **5**, 6249–6254 (2015).
10. B. Liu *et al.*, Reaction dynamics of CN radicals in acetonitrile solutions. *J. Phys. Chem. A* **119**, 12923–12934 (2015).
11. Q. Fu *et al.*, Interface-confined ferrous centers for catalytic oxidation. *Science* **328**, 1141–1144 (2010).
12. G. Chen *et al.*, Interfacial effects in iron-nickel hydroxide-platinum nanoparticles enhance catalytic oxidation. *Science* **344**, 495–499 (2014).
13. S. Chen *et al.*, Anchoring high-concentration oxygen vacancies at interfaces of CeO(2–x)/Cu toward enhanced activity for preferential CO oxidation. *ACS Appl. Mater. Interfaces* **7**, 22999–23007 (2015).
14. Q. Fu, F. Yang, X. Bao, Interface-confined oxide nanostructures for catalytic oxidation reactions. *Acc. Chem. Res.* **46**, 1692–1701 (2013).
15. L. Xu, Y. Ma, Y. Zhang, Z. Jiang, W. Huang, Direct evidence for the interfacial oxidation of CO with hydroxyls catalyzed by Pt/oxide nanocatalysts. *J. Am. Chem. Soc.* **131**, 16366–16367 (2009).
16. Y. Zhao *et al.*, Stable iridium dinuclear heterogeneous catalysts supported on metal-oxide substrate for solar water oxidation. *Proc. Natl. Acad. Sci. U.S.A.* **115**, 2902–2907 (2018).
17. K. R. Yang *et al.*, Solution structures of highly active molecular Ir water-oxidation catalysts from density functional theory combined with high-energy X-ray scattering and EXAFS spectroscopy. *J. Am. Chem. Soc.* **138**, 5511–5514 (2016).
18. Y. Huang, A. Wang, X. Wang, T. Zhang, TMS06: Symposium on materials in clean power systems. *Int. J. Hydrogen Energy* **32**, 3880–3886 (2007).
19. J. Lin *et al.*, Design of a highly active Ir/Fe(OH)x catalyst: Versatile application of Pt-group metals for the preferential oxidation of carbon monoxide. *Angew. Chem. Int. Ed. Engl.* **51**, 2920–2924 (2012).
20. L. Nie *et al.*, Activation of surface lattice oxygen in single-atom Pt/CeO2 for low-temperature CO oxidation. *Science* **358**, 1419–1423 (2017).
21. D. Widmann, R. J. Behm, Active oxygen on a Au/TiO2 catalyst: Formation, stability, and CO oxidation activity. *Angew. Chem. Int. Ed. Engl.* **50**, 10241–10245 (2011).
22. L. B. Vilhelmsen, B. Hammer, Interfacial oxygen under TiO2 supported Au clusters revealed by a genetic algorithm search. *J. Chem. Phys.* **139**, 204701 (2013).
23. L. DeRita *et al.*, Structural evolution of atomically dispersed Pt catalysts dictates reactivity. *Nat. Mater.* **18**, 746–751 (2019).
24. R. Bliem *et al.*, Dual role of CO in the stability of subnano Pt clusters at the Fe3O4(001) surface. *Proc. Natl. Acad. Sci. U.S.A.* **113**, 8921–8926 (2016).
25. L. Vaska, J. W. DiLuzio, Carbonyl and hydrido-carbonyl complexes of iridium by reaction with alcohols. Hydrido complexes by reaction with acid. *J. Am. Chem. Soc.* **83**, 2784–2785 (1961).
26. H. J. Lawson, J. D. Atwood, Oxygen atom transfer from an iridium dioxygen complex: Oxidation of carbon monoxide to carbonate. *J. Am. Chem. Soc.* **110**, 3680–3682 (1988).
27. C. J. Cramer, W. B. Tolman, K. H. Theopold, A. L. Rheingold, Variable character of O-O and M-O bonding in side-on (eta(2)) 1:1 metal complexes of O2. *Proc. Natl. Acad. Sci. U.S.A.* **100**, 3635–3640 (2003).